

Original Research

Sparc Suppresses Microglial Neuroinflammation and Promotes Axonal Regeneration by Interacting With Uba52

Hangyu Ji^{1,2}, Kun Wang³, Yili Hu², Yefu Xu², Jiangkai Yu², Chengming Li^{1,*}

Academic Editor: Thomas Heinbockel

Submitted: 21 May 2025 Revised: 4 August 2025 Accepted: 11 August 2025 Published: 21 August 2025

Abstract

Background: After spinal cord injury (SCI), pro-inflammatory microglia accumulate and impede axonal regeneration. We explored whether secreted protein acidic and rich in cysteine (Sparc) restrains microglial inflammation and fosters neurite outgrowth. Methods: Mouse microglial BV2 cells were polarized to a pro-inflammatory phenotype with lipopolysaccharides (LPSs). Sparc mRNA and protein were quantified by reverse transcription quantitative PCR (RT-qPCR). Sparc was overexpressed via plasmid transfection, then inflammatory cytokines, mitochondrial membrane potential ($\Delta\Psi$ m), reactive oxygen species (ROS), and oxidative-phosphorylation proteins, including voltage-dependent anion channel 1 (VDAC1), cytochrome c oxidase subunit 1 (COX1), and ATP synthase α subunit (ATP5A), were assayed by Western blot, enzyme-linked immunosorbent assay (ELISA), and flow cytometry. Immunoprecipitation plus mass spectrometry, co-immunoprecipitation, and immunofluorescence confirmed the interaction between Sparc and ubiquitin A-52 residue ribosomal protein fusion product 1 (Uba52). Effects of Sparc overexpression alone or combined with Uba52 small interfering RNA (si-Uba52) were compared in LPS-induced BV2 cells. Finally, BV2 cells and a mouse hippocampal neuron (HT-22) were co-cultured in the Transwell chamber, and the changes in proliferation, apoptosis, and III-tubulin content of the latter were detected. Results: In LPS-induced BV2 cells, the tumor necrosis factor- α (TNF- α), interleukin-6 (IL-6), and ROS levels were elevated, while the IL-10 and transforming growth factor- β (TGF- β) levels, $\Delta\Psi$ m, and the proteins levels of the VDAC1, COX1, ATP5A, and Sparc decreased. Sparc overexpression reversed these changes. Mechanistically, Sparc bound Uba52 and upregulated its expression; Uba52 knockdown abolished the anti-inflammatory and mitochondrial-protective effects of Sparc. In co-culture, Sparc overexpression rescued HT-22 neurons apoptosis and enhanced axonal growth, but the effects were also reversed by Uba52 knockdown. Conclusions: Sparc may maintain mitochondrial homeostasis by interacting with Uba52 to inhibit LPS-induced BV2 inflammatory response, thereby promoting neuronal axonal regeneration. This suggests that Sparc may play a potential role in SCI repair.

Keywords: spinal cord injury; microglial; inflammation; axonal regeneration; Sparc; Uba52

1. Introduction

Spinal cord injury (SCI) involves complete or partial disruption of spinal cord structural integrity and neurological functions resulting from traumatic or non-traumatic pathogenic factors, precipitating pathological cascades characterized by neuronal loss and axonal rupture [1-3]. In the acute phase following SCI, resident microglia are rapidly recruited and activated at the lesion site. Functionally distinct microglial subtypes emerge: pro-inflammatory microglia drive neurotoxic effects including amplified neuroinflammation, heightened neuronal death, and aggravated tissue damage, whereas anti-inflammatory microglia enhance neural tissue tolerance, mediate blood-spinal cord barrier repair, support neurovascular regeneration, and restore microenvironmental homeostasis [4,5]. Within hours post-injury, pathological stimuli trigger microglial polarization. Persistent exposure to the dysregulated microenvironment subsequently promotes progressive dominance of proinflammatory microglial populations. While suppression of pro-inflammatory microglial expansion has been shown to improve neurological recovery post-SCI, the precise regulatory mechanisms remain poorly defined [6,7].

Emerging evidence implicates mitochondria as central signaling platforms that govern immune cell phenotypic specification and modulate microglial inflammatory responses [8]. Mitochondrial dysfunction during neuroinflammation critically alters microglial metabolic states, thereby influencing inflammatory progression. Our prior work revealed concurrent activation of mitophagy during microglial polarization, with experimental manipulation of mitophagic flux directly modulating phenotypic switching [9].

Secreted protein acidic and rich in cysteine (Sparc), a matricellular protein, regulates cytokine activity, extracellular matrix dynamics, and tissue repair processes. During central nervous system (CNS) development, Sparc is abundantly expressed in microglia, yet its expression diminishes significantly in mature CNS microglia [10]. Sparc

¹Department of Spine Surgery, Zhongda Hospital Southeast University, 210009 Nanjing, Jiangsu, China

²Medicine School, Southeast University, 210009 Nanjing, Jiangsu, China

³Department of Spine Surgery, Shanghai Sixth People's Hospital, 201306 Shanghai, China

^{*}Correspondence: lichengming666@163.com (Chengming Li)

deficiency has been demonstrated to exacerbate microglial macrophage activation [11,12], suggesting its potential role in constraining pro-inflammatory phenotypic conversion. To address current knowledge gaps, this study investigates *Sparc*-mediated regulation of pro-inflammatory microglial activation, delineates underlying molecular mechanisms, and evaluates its neuroprotective effects through suppression of microglial-driven neuroinflammation. These findings may advance therapeutic strategies for axonal regeneration and functional recovery following SCI.

2. Materials and Methods

2.1 Cell Culture

BV2 microglial cells were cultured in RPMI-1640 medium supplemented with 10% fetal bovine serum (FBS) and 1% penicillin-streptomycin. HT-22 neuronal cells were maintained in high-glucose dulbecco's modified eagle medium (DMEM) containing 10% FBS. Subculture protocol: After aspirating the spent medium, cells were gently washed twice with 37 °C pre-warmed PBS, followed by digestion with 0.25% Trypsin-EDTA (45 seconds for BV2; 2.5 minutes for HT-22). Upon observation of intercellular gap widening under a microscope, serum-containing medium was added to neutralize trypsin. Cells were collected by centrifugation at 1000 rpm for 5 minutes and subcultured at a 1:3 ratio. Complete medium replacement was performed every 2 days, with cell density maintained between 30% and 80%. BV2 and HT-22 cells were purchased from Jiangsu KeyGENE Technology Co., Ltd. (Nanjing, China). All cell lines were validated by short tandem repeat (STR) profiling and tested negative for mycoplasma.

2.2 Cell Transfection and Induction

The Sparc coding DNA sequence (CDS) region sequence was searched through the national center for biotechnology information (NCBI) online website (https: //www.ncbi.nlm.nih.gov/), and the CDS region sequence was imported into pcDNA3.1 expression plasmid to construct the Sparc overexpression recombinant plasmid. Sparc overexpression plasmid and Uba52 small interfering RNA (si-Uba52) sequences were synthesized by Key-GEN BioTECH Co., Ltd. (KeyGEN Biotech, Nanjing, China). When the fusion degree of BV2 cells reached about 70%, the cells were divided into 3 groups: control, lipopolysaccharides (LPS), and LPS + Sparc. Cells in the LPS group were treated with 200 ng/mL LPS (Sigma, St. Louis, MO, USA) for 24 hours. LPS + Sparc cells were transfected with Sparc overexpression plasmid by Lipofectamine 3000 (Thermo Fisher, Waltham, MA, USA), cultured for 24 hours and then treated with 200 ng/mL LPS for 24 hours. Cells in the control group were cultured normally for 24 hours.

In addition, the cells were divided into three groups again: LPS, LPS + *Sparc*, and LPS + *Sparc* + si-*Uba52*. Cells in the LPS and LPS + *Sparc* groups were treated as

above. Cells in the LPS + *Sparc* + si-*Uba52* group were co-transfected with the *Sparc* overexpression plasmid and si-*Uba52* by Lipofectamine 3000. After 24 hours of culture, cells were treated with 200 ng/mL LPS for 24 hours.

2.3 Co-Immunoprecipitation Coupled Mass Spectrometry

Lysis conditions: 1×10^7 cells were collected and lysed in pre-cooled radioimmunoprecipitation assay (RIPA) buffer (containing 1% NP-40, 0.5% sodium deoxycholate, 0.1% sodium dodecyl sulfate (SDS), and protease inhibitors) on ice for 30 minutes, with vortexing for 5 seconds every 10 minutes. After centrifugation at $14,000 \times g$ for 15 minutes, the supernatant was collected, and protein concentration was quantified using the bicinchoninic acid (BCA) assay.

Immunoprecipitation: 1 mg total protein was incubated with Sparc antibody overnight at 4 °C with rotation, followed by 4 hours of incubation with Protein G agarose beads. Beads were washed 5 times with lysis buffer, and bound proteins were eluted using low-pH elution buffer. Target bands excised from sodium dodecyl sulfate-polyacrylamide gel electrophoresis (SDS-PAGE) gels were trypsin-digested at 37 °C for 16 hours for subsequent mass spectrometry analysis.

2.4 Mitochondrial Membrane Potential Assay (JC-1)

The transfected cells and untransfected cells were digested, counted, and prepared into cell a suspension with a concentration of 1×10^5 cells/mL, and inoculated into a six-well plate. The next day, after the cells were attached, the corresponding medium containing 200 ng/mL LPS was added according to the group setting, and a negative control group was set up. After 24 hours of drug treatment, the cells were digested with 0.25% trypsin (without EDTA) and collected. The cells were washed once with PBS (centrifuged at 1000 rpm for 5 minutes) and the cell concentration was adjusted to 1×10^6 /mL. The cells were evenly suspended with 500 µL of prepared JC-1 working solution and incubated in an incubator at 37 °C with 5% CO2 for 15-20 minutes. Cells were collected by centrifugation at room temperature (1000 rpm for 5 minutes) and washed twice with $1\times$ Incubation Buffer. The cells were resuspended by absorbing 500 μ L of 1 \times Incubation Buffer. Test on the machine.

2.5 Reactive Oxygen Species (ROS) Analysis

The transfected cells and untransfected cells were digested, counted, and prepared into a cell suspension with a concentration of 1×10^5 cells/mL, and inoculated into a six-well plate. The next day, after the cells were attached, the corresponding medium containing 200 ng/mL LPS was added according to the group setting, and a negative control group was set up. After 24 hours of drug treatment, the cells were digested with 0.25% trypsin (without EDTA) and collected. The cells were washed once with PBS (centrifuged at 1000 rpm for 5 minutes) and the cell concentration was



adjusted to $1 \times 10^6/\text{mL}$. 2',7'-Dichlorofluorescin diacetate (DCFH-DA) was diluted in serum-free medium at 1:1000 to a final concentration of 10 μ M. The cells were collected and suspended in the diluted DCFH-DA and incubated in a cell incubator at 37 °C for 20 minutes. The probe was mixed reversely every 3–5 minutes to make full contact with the cells. The cells were washed 3 times with serum-free cell culture medium to fully remove DCFH-DA that did not enter the cells. Flow cytometry was used to detect (Ex = 488 nm; Em = 525 nm).

2.6 Reverse Transcription Quantitative PCR (RT-qPCR)

After centrifugation, the colorless supernatant water was drawn and transferred to another centrifuge tube. After centrifugation, an equal volume of isopropanol and 70% ethanol was added. After centrifugation, RNase-free water was added to dissolve the RNA precipitation. After the concentration and purity of RNA were determined, 0.2 mL polymerase chain reaction (PCR) tubes that had been sterilized and had no nuclease were taken, and RNA (2 µg), $5\times$ PrimeScript RT Master Mix (Takara Bio Inc., Kyoto, Japan, RR036B) were added in turn, and the products were obtained by centrifugation. The cDNA samples were diluted and TB Green® Premix Ex Taq^TM The II (Tli RNaseH Plus) reagent (Takara, Japan, RR820A) contains $2\times$ Realtime PCR Master Mix, SYBR Green, template, and primer Mix were successively added to 0.1 mL PCR tubes.

2.7 Western Blot

Cells were collected, lysates were added, protein samples were extracted, protein concentration was calculated according to the standard curve, 10% SDS-PAGE gel was prepared, electrophoresed, transferred to polyvinylidene fluoride (PVDF) membrane, blocked with 1% bovine serum albumin (BSA) for 1 hour, added primary antibody, incubated at 4 °C overnight, wash with PBS, add secondary antibody and incubate at room temperature for 2 hours. The obtained bands were imaged by ChemiDoc MP Imaging System 3.0.1 version (Bio-Rad, Hercules, CA, USA), and the gray level was analyzed by the Gel-Pro32 software 6.0 version (Media Cybernetics, Inc., Rockville, MD, USA).

2.8 Enzyme-Linked Immunosorbnent Assay (ELISA)

The kits (Tumor necrosis factor- α (TNF- α) kit: Mlbio, Shanghai, China, YJ002095; Interleukin-6 (IL-6) kit: Mlbio, Shanghai, China, YJ063159; Transforming growth factor- β (TGF- β) kit: Mlbio, Shanghai, China, YJ057830; Interleukin-10 (IL-10) kit: Mlbio, Shanghai, China, YJ037873) were operated according to the instructions of each kit. The original standard substance was diluted in an EP tube, and through the process of adding sample, adding enzyme, incubation, mixing, washing, and color development, the absorbance (OD) value of each well was measured at 450 nm wavelength 15 minutes after adding the termination solution.

2.9 Co-culture in Transwell Chambers

Co-culture of BV2 cells and HT-22 cells was performed using Transwell chambers. BV2 cells were seeded in the upper chamber of Transwell, and HT-22 cells were seeded in 24-well plates. The co-culture cells were divided into 4 groups: Control/HT-22, LPS/HT-22, LPS + *Sparc*/HT-22, LPS + *Sparc* + si-*Uba52*/HT-22. BV2 cells in each group were treated as above and co-cultured with HT-22 cells for 24 hours.

2.10 EdU Proliferation Assay

24 hours after transfection, BV2 cells were digested, counted, and prepared into a cell suspension with a concentration of 1×10^4 cells/mL. A total of 200 μ L cell suspension was added to each well of the 24-well cell co-culture upper chamber, and HT-22 cells in logarithmic growth phase were digested, counted, and prepared into a cell suspension with a concentration of 1×10^4 cells/mL. An amount of 800 µL of HT-22 cell suspension was added to each well in the lower chamber. After cell attachment, the co-cultured cells were treated with 200 ng/mL LPS for an additional 24 hours. The lower layer of HT-22 cells was removed, the medium was discarded, and the cells were washed twice with PBS. EdU (medium preparation 50 μM), 500 µL cell fixative (i.e., PBS containing 4% paraformaldehyde), 200 μL 2 mg/mL glycine, 500 μL PBS, 1× Apollo® staining reaction solution, and 500 µL osmotic agent (0.5% TritonX-100 in PBS) were added sequentially to cells in each well and 500 µL of 1× Hoechst 33342 reaction solution was prepared prior. After washing with PBS, the plates were sealed, and the pictures were taken under a fluorescence microscope (200×) (Olympus, Tokyo, Japan).

2.11 Annexin V-APC/Propidium Iodide (PI) Apoptosis Assay

The co-cultured HT-22 cells were collected by 0.25% trypsin (without EDTA) digestion. Cells were washed twice with PBS (centrifuged at 1000 rpm for 5 minutes) to collect 1×10^6 cells. A total of 500 μL Binding Buffer was added to suspend the cells. After 5 μL Annexin V-APC was added to the mix, 5 μL Propidium Iodide was added to the mix. The reaction time was 5–15 minutes at room temperature in the dark. Cell apoptosis was detected by flow cytometry.

2.12 Immunofluorescence

The lower layer of HT-22 cells was removed, the medium was discarded, and the cell samples were allowed to dry naturally. The cells were immersed in 4% paraformaldehyde fixator for 30 min or overnight to improve cell permeability, and the cells were immersed in PBS for 3 minutes \times 3. The cells were covered with 3% $\rm H_2O_2-$ methanol solution and blocked at room temperature (15–25 °C) for 10 minutes. After soaking with PBS three times, 100 μL of ready-to-use goat serum was added and incubated at room temperature for 20 minutes. Then 100 μL of



rabbit anti-III-tubulin (Abclonal, Wuhan, China, A17913, 1:50), FITC-labeled goat anti-rabbit IgG-HRP (KeyGEN Biotech, Nanjing, China, KGC6214-0.1, 1:5000), and prepared Hoechst staining solution were added in turn, placed in a dark place at room temperature for 5 minutes, and washed 3 times with PBS. A total of 1 mL PBS was added and the expression was observed under a confocal microscope (Olympus, Tokyo, Japan). Three highly expressed regions were taken and photographed, and stored (600×).

For dual-colour immunofluorescence co-localisation of Uba52 and Sparc, BV2 cells seeded on glass coverslips were fixed with 4% paraformaldehyde for 30 minutes, permeabilised with 0.2% Triton X-100, and blocked with 3% BSA for 30 minutes. Sequential tyramide signal amplification (TSA) labelling was performed on the same slide. First, rabbit anti-Uba52 (Abclonal, Wuhan, China, A20876, 1:500) was applied overnight at 4 °C, followed by goat anti-rabbit IgG-HRP (KeyGEN Biotech, Nanjing, China, KGC6202, 1:5000) and Alexa Fluor 488-TSA. After stringent antibody elution (37 °C, 15-30 minutes in citrate-based buffer), the second cycle was executed with rabbit anti-Sparc (Proteintech, Wuhan, China, 15274-1-AP, 1:1000), identical HRP-secondary and Alexa Fluor 594-TSA. Nuclei were counterstained with 4',6-Diamidino-2'phenylindole (DAPI). Coverslips were mounted with antifade medium and imaged on a confocal laser-scanning microscope (Olympus, Tokyo, Japan).

2.13 Statistical Analysis

All experimental data are presented as mean \pm standard deviation. One-way analysis of variance (ANOVA) was used for comparison among multiple groups, and the LSD method was used for post hoc comparison. Statistical software SPSS (ver. 23.0, IBM, Beijing, China), the error line represents the standard deviation of three independent means, *p < 0.05; **p < 0.01; ***p < 0.01.

3. Results

3.1 Sparc Overexpression Suppresses Pro-Inflammatory Responses and Regulates Mitochondrial Homeostasis in LPS-Induced BV2 Cells

Mitochondrial dysfunction during neuroinflammation exacerbates inflammatory progression by reprogramming microglial metabolism. In LPS-induced BV2 cells. *Sparc* overexpression significantly restored mitochondrial membrane potential (Fig. 1A), attenuated ROS production (Fig. 1B), and upregulated mitochondrial oxidative phosphorylation (mt-OXPHOS)-related proteins voltage-dependent anion channel 1 (VDAC1), cytochrome c oxidase subunit 1 (COX1), and ATP synthase α subunit (ATP5A) (Fig. 1C). Besides, LPS induction markedly increased pro-inflammatory cytokines TNF- α and IL-6 while suppressing anti-inflammatory mediators IL-10 and TGF- β , which were reversed by *Sparc* overexpression (Fig. 1D).

3.2 Sparc Interacts With Uba52 and Positively Regulates Its Expression

Immunoprecipitation combined with mass spectrometry confirmed potential binding between Sparc and Uba52 (Fig. 2A,B). Subsequently, the interaction of the Sparc-Uba52 was confirmed through colocalization of co-immunoprecipitation and immunofluorescence (Fig. 2C,D). LPS stimulation suppressed both *Uba52* mRNA and protein levels, whereas *Sparc* overexpression rescued its expression (Fig. 2E,F).

To knockdown *Uba52* in BV2 cells, three si-*Uba52* were designed. The verification results of RT-qPCR showed that si-*Uba52*#02 had the best inhibition rate on the expression of the *Uba52* gene (Fig. 2G). Therefore, si-*Uba52*#02 was selected for the *Uba52* knockdown experiment. *Uba52* knockdown reduced the *Uba52* gene and protein without altering the *Sparc* gene and protein expressions (Fig. 2F,H,I), establishing Uba52 as a downstream effector of Sparc.

3.3 The Sparc-Uba52 Axis May Attenuate Microglial Inflammation Via Mitochondrial Respiration Control

Sparc overexpression reversed LPS-induced mitochondrial depolarization (Fig. 3A) and restored VDAC1, COX1, and ATP5A expressions (Fig. 3C), effects abolished by Uba52 knockdown. Sparc suppressed ROS accumulation (Fig. 3B), whereas Uba52 knockdown exacerbated it. Sparc overexpression inhibited TNF- α and IL-6 levels and enhanced IL-10 and TGF- β expression, while Uba52 knockdown neutralized these anti-inflammatory effects (Fig. 3D).

3.4 Sparc-Uba52 Interaction Promotes Axonal Regeneration Through Microglial Immunomodulation

Transwell co-culture assays demonstrated that proinflammatory BV2 supernatants strongly inhibited HT-22 neuronal proliferation (Fig. 4A,B). *Sparc* overexpression rescued neuronal proliferation (Fig. 4B), whereas si-*Uba52* intensified suppression. Apoptosis analysis revealed that *Sparc* attenuated LPS-induced neuronal apoptosis (Fig. 4C), while *Uba52* silencing amplified cell death (Fig. 4C). III-tubulin expression patterns corroborated these findings: *Sparc* restored neurite outgrowth capacity, whereas si-*Uba52* diminished it (Fig. 4D).

4. Discussion

This study elucidates a mechanism by which Sparc interacts with the ribosomal ubiquitination modifier Uba52 to maintain mitochondrial functional homeostasis and inhibit inflammation in LPS-induced BV2 cells, ultimately modulating neuronal function. Our findings reveal a previously unrecognized immunometabolic crosstalk network in neuroinflammatory regulation.

Our findings demonstrate that Sparc interacts with Uba52 to form a functional complex and upregulates *Uba52*



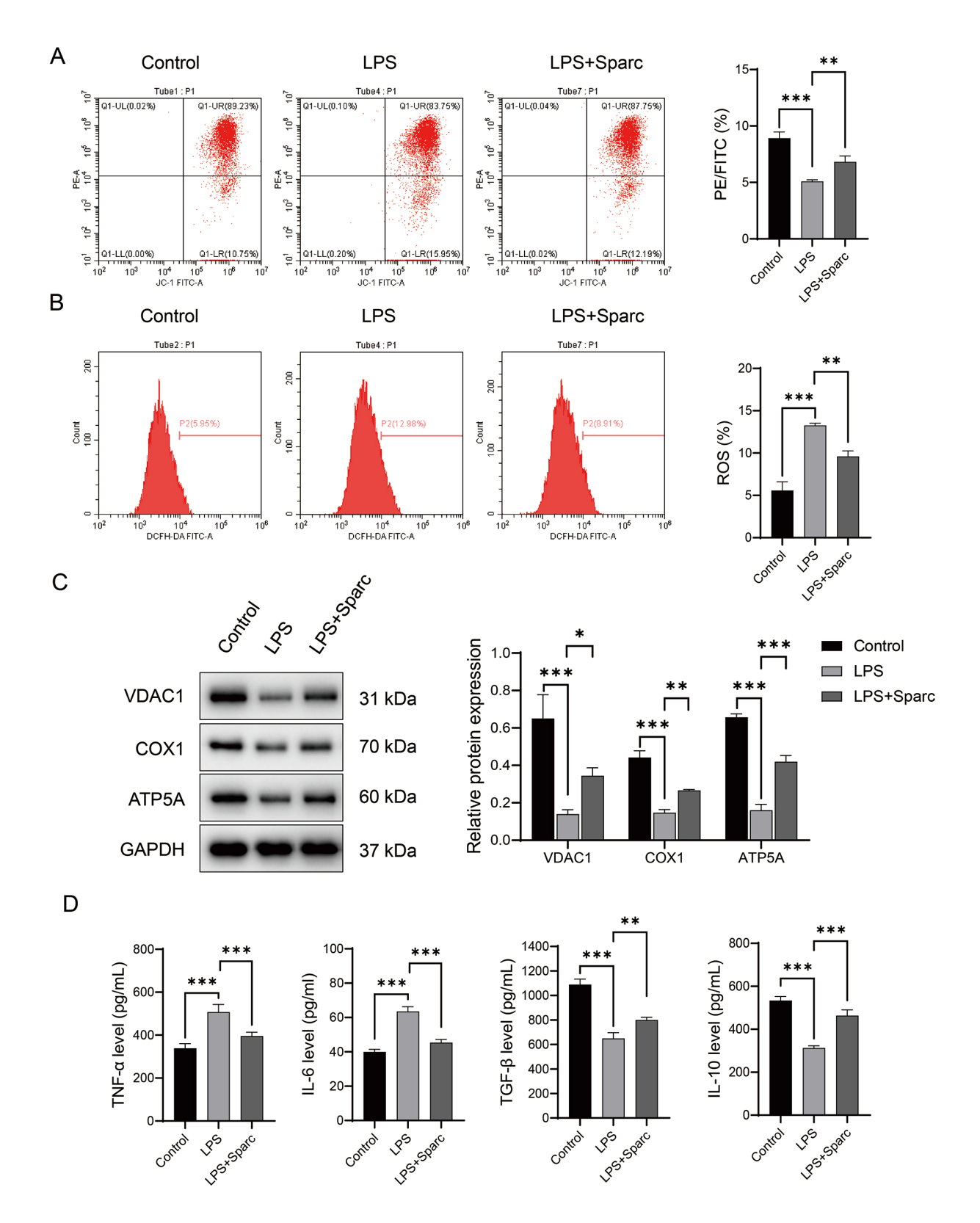


Fig. 1. Sparc overexpression suppresses pro-inflammatory responses and regulates mitochondrial homeostasis in lipopolysac-charides (LPS)-induced BV2 cells. (A) JC-1 method for detecting mitochondrial membrane potential. (B) 2',7'-Dichlorofluorescin diacetate (DCFH-DA) probe for detecting reactive oxygen species (ROS) levels. (C) Western blot detection of mitochondrial functional proteins (voltage-dependent anion channel 1 (VDAC1), cytochrome c oxidase subunit 1 (COX1), ATP synthase α subunit (ATP5A)). (D) Enzyme-linked immunosorbent assay (ELISA) detection of cytokine levels (TNF- α , IL-6, TGF- β , IL-10). *p < 0.05, **p < 0.01, and ***p < 0.001. TNF- α , tumor necrosis factor- α ; IL-6, interleukin-6; TGF- β , transforming growth factor- β .

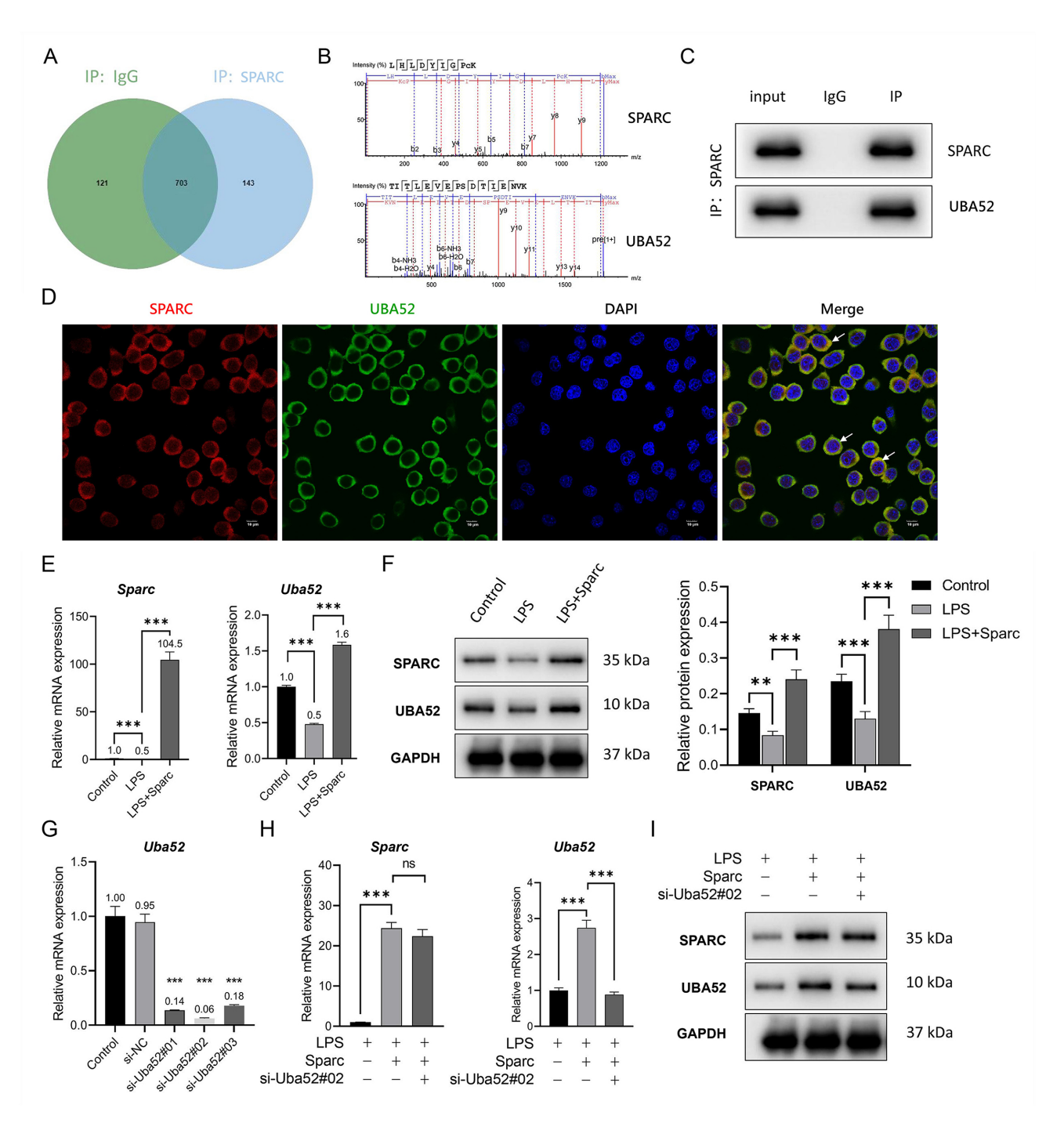


Fig. 2. Spare interacted with Uba52 and promoted *Uba52* expression. (A–C) The interaction between Spare and Uba52 protein was confirmed through co-immunoprecipitation coupled mass spectrometry. Input: 10% total lysate; Ig G: negative control; IP: anti-Spare immunoprecipitated. (D) Co-localization analysis of the Spare and Uba52 was performed using immunofluorescence. The white arrow represents the co-localization area, where yellow (red and green overlapping) indicates spatial overlap between Spare and Uba52. Scale bar: $10 \,\mu\text{m}$. (E,F) Changes in expression levels of the *Spare* and *Uba52* genes and proteins in BV2 cells under the intervention of *Spare* overexpression. (G) *Uba52* knockdown validation was conducted using RT-qPCR. (H,I) Expression changes of the *Spare* and *Uba52* genes and proteins after transfection of si-*Uba52* in BV2 cells. **p < 0.01, ***p < 0.001, and ns: p > 0.05.

expression. Notably, while *Uba52* is conventionally recognized as a ubiquitin precursor protein involved in ribosomal ubiquitination and protein quality control, this study unveils its potential role in mitochondrial function regulation.

Specifically, Sparc can increase mitochondrial membrane potential and the expression of mt-OXPHOS-related proteins, and reduce the production of ROS and inflammation in LPS-induced BV2 cells. Critically, *Uba52* knockdown



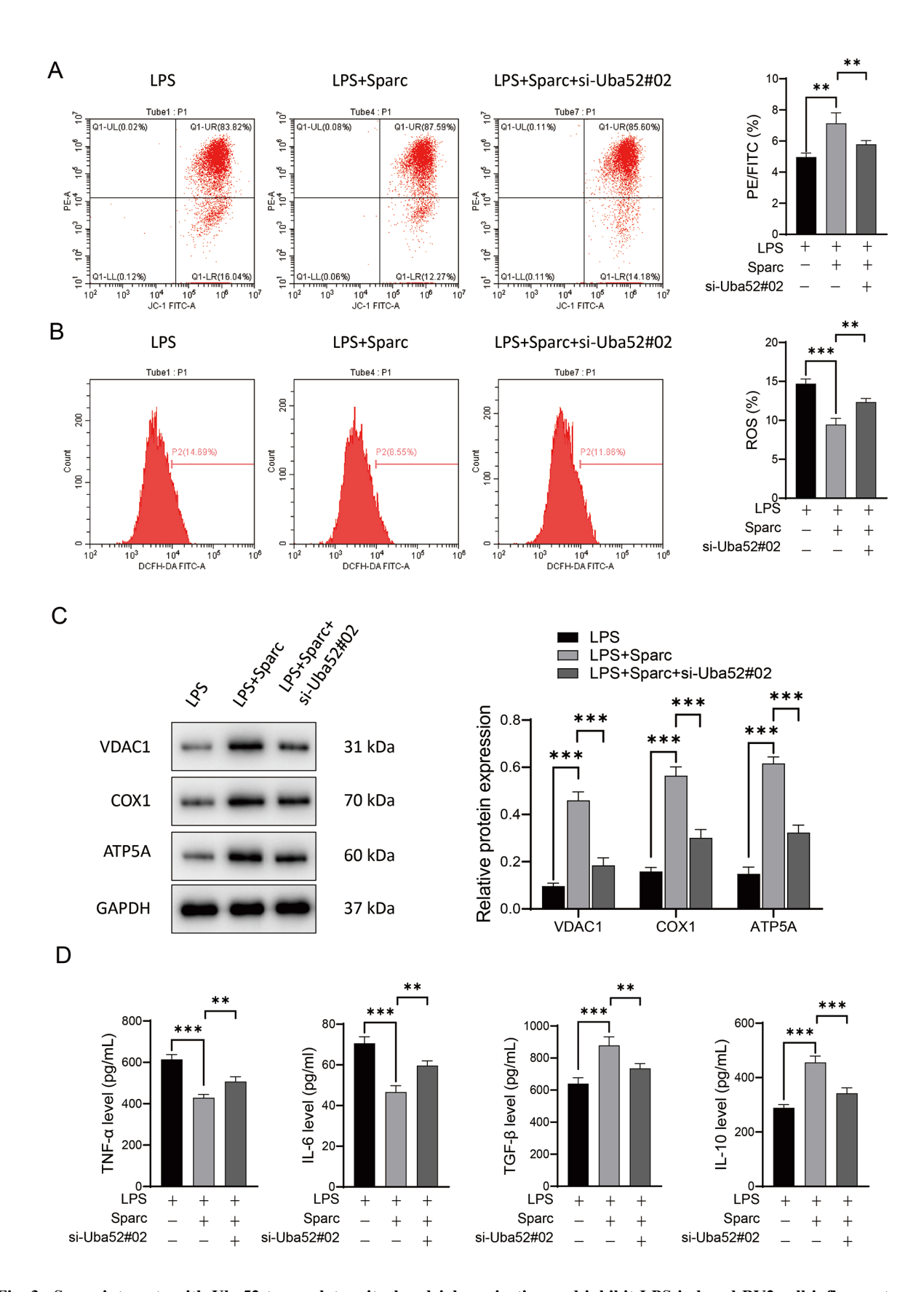


Fig. 3. Spare interacts with Uba52 to regulate mitochondrial respiration and inhibit LPS-induced BV2 cell inflammatory responses. (A) Mitochondrial membrane potential measured by JC-1 assay. (B) Intracellular ROS levels detected by DCFH-DA probe. (C) Western blot analysis of mitochondrial respiratory chain proteins (VDAC1, COX1, ATP5A). (D) mRNA levels of inflammatory factors by qPCR. **p < 0.01, ***p < 0.001.

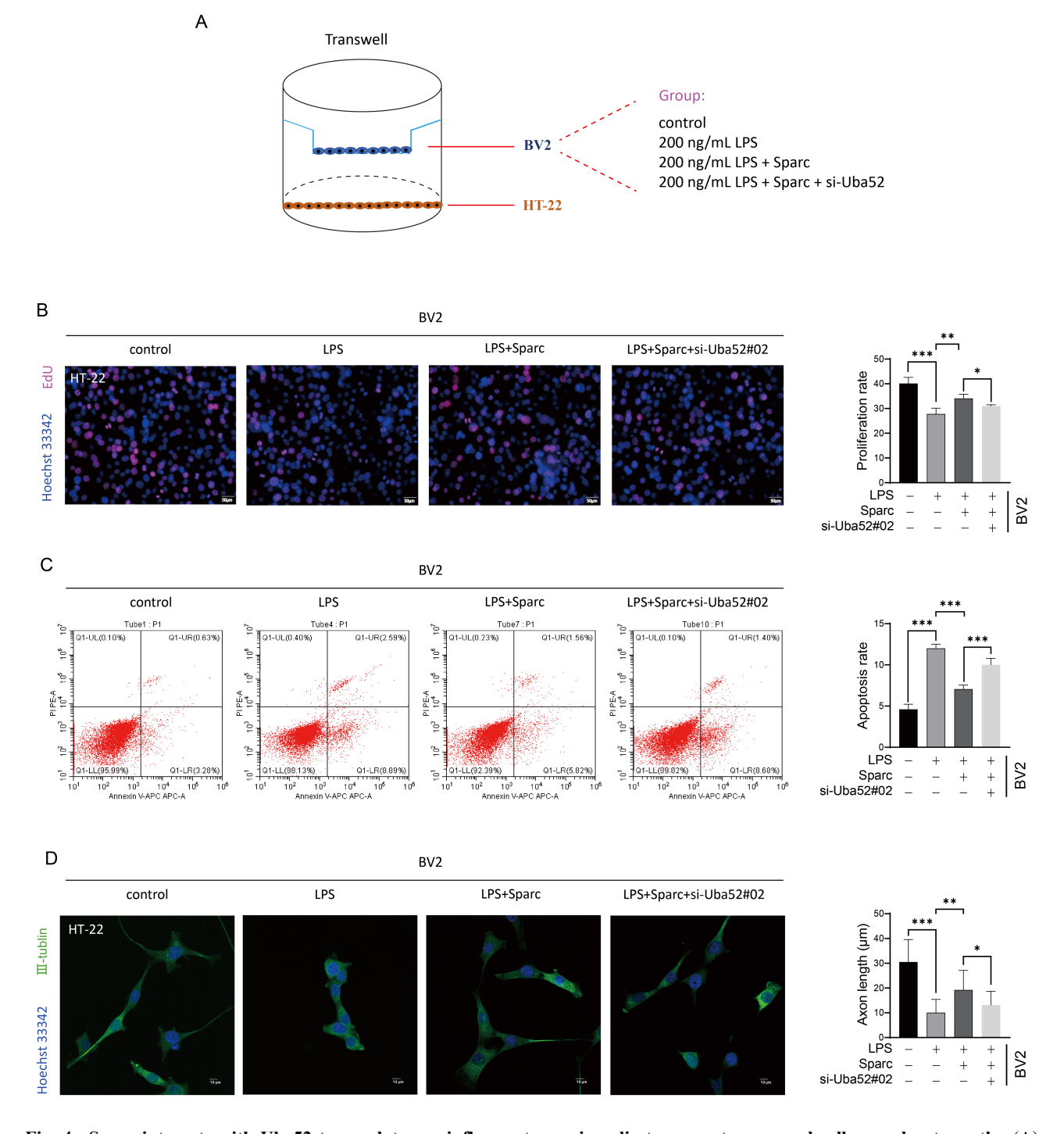


Fig. 4. Sparc interacts with Uba52 to regulate pro-inflammatory microglia to promote neuronal cell axonal outgrowth. (A) Schematic diagram of Transwell co-culture system. Created by Adobe Illustrator 2022. (B) Quantification of HT-22 neuronal proliferation under different treatments. Left panels: Representative images of EdU staining (red, proliferating cells) and Hoechst 33342 (blue, nuclei). Scale bar: 50 μ m. (C) Annexin V-APC/Propidium Iodide (PI) dual staining was used to detect apoptosis. (D) Quantification of axonal outgrowth in HT-22 neurons by III-tubulin immunofluorescence. Left panels: Representative confocal images of III-tubulin (green) and nuclei (blue, Hoechst). Scale bar: $10~\mu$ m. *p < 0.05, **p < 0.01, and ***p < 0.001.

partially abrogates *Sparc*-mediated protection of mitochondrial function and anti-inflammatory effect. It is reported that when macrophages transform into pro-inflammatory types, mitochondrial function changes, including OXPHOS

and mitochondrial membrane potential decrease, while the production of ROS increases [13]. This metabolicinflammatory coupling mirrors the "Warburg effect" observed in pro-inflammatory macrophages, where glycolytic



flux predominates over oxidative phosphorylation for energy production [14,15]. These studies suggest that Sparc may maintain mitochondrial functional homeostasis by interacting with Uba52 to inhibit the pro-inflammatory response of LPS-induced BV2 cells.

Although *Sparc* intervention significantly reduces total ROS levels, subcellular localization analysis is required to determine whether this reduction specifically targets mitochondrial ROS. Furthermore, the observed upregulation of ATP5A may enhance OXPHOS efficiency, potentially providing the energetic foundation necessary for anti-inflammatory polarization [16].

The study further reveals that pro-inflammatory BV2 cells suppress axonal growth in HT-22 neurons, a phenomenon closely mirroring the "chronic neuroinflammation-neuronal injury" vicious cycle characteristic of neurodegenerative pathologies. We propose that Sparc promotes neuronal repair via dual mechanisms: (1) Direct metabolic regulation: The Sparc-Uba52 complex sustains mitochondrial homeostasis and reduces pro-inflammatory cytokine (TNF- α and IL-6) release. Notably, TNF- α has been shown to induce neuronal apoptosis via receptor-interacting protein kinase 1 (RIPK1) pathway activation [17]. (2) Indirect trophic support: Microglia with preserved mitochondrial function could secrete increased tricarboxylic acid cycle metabolites, directly bolstering neuronal energy metabolism and axon Crucially, Uba52 knockdown partially regeneration. abolishes Sparc-mediated neuroprotection, identifying this axis as a potential therapeutic target to disrupt the neuroinflammation-neuronal damage cycle.

Moreover, conventional paradigms posit that microglial phenotypic switching is coordinately regulated by multiple signaling pathways [18]. Our study reveals that the Sparc-Uba52 axis independently governs metabolic reprogramming, suggesting the existence of parallel regulatory mechanisms. Extending the concept of mitochondria as immunometabolic regulators where mitochondrial-derived mitochondrial DNA (mtDNA) and ROS are known to activate the NOD-like receptor thermal protein domain associated protein 3 (NLRP3) inflammasome [19], this work identifies respiratory chain integrity itself as an inflammationsuppressive signal. While Uba52 typically participates in protein degradation, our findings demonstrate its protective role through mitochondrial protein stabilization, providing novel evidence supporting the emerging paradigm of bidirectional regulatory capacity in ubiquitination modifications.

Although this study revealed the potential mechanism by which the Sparc–Uba52 axis inhibits microglial inflammation by maintaining mitochondrial functional homeostasis, the following key issues still need further validation: (1) Further research is needed to determine whether the effect of Sparc–Uba52 axis on mitochondrial protein expression depends on ROS clearance without the use of antioxidants

such as Mito-TEMPO; (2) In addition to inflammatory factors, the toll-like receptor 4 (TLR4) mediated inflammatory pathway plays an important role in the pro-inflammatory response and ROS of microglia. Subsequently, Western blot will be used to detect the expression of key proteins on the toll-like receptor 4/myeloid differentiation factor 88/nuclear factor- κ B (TLR4/MyD88/NF- κ B) pathway to clarify the effect of the Sparc–Uba52 axis on the activation of the TLR4/MyD88/NF- κ B pathway; (3) In the future, the neuroprotective efficacy and mechanism specificity of the Sparc–Uba52 axis will be further validated through *Sparc* gene intervention in animal models of SCI.

5. Conclusions

To sum up, this study demonstrates that Sparc modulates mitochondrial respiration and suppresses microglial pro-inflammatory responses through its interaction with Uba52, further promoting axonal regeneration. We initially elucidate the potential mechanisms by which the Sparc–Uba52 axis governs microglial inflammatory phenotype. These findings identify potential therapeutic targets for SCI.

Availability of Data and Materials

The datasets used or analyzed during the current study are available from the corresponding author on reasonable request.

Author Contributions

HJ conducted experimental design, data analysis, and wrote this article. KW conducted experimental design. YH, YX and JY conducted experimental operations and data analysis. CL conducted experimental design, wrote this article and revised the manuscript. All authors contributed to editorial changes in the manuscript. All authors read and approved the final manuscript. All authors have participated sufficiently in the work and agreed to be accountable for all aspects of the work.

Ethics Approval and Consent to Participate

Not applicable.

Acknowledgment

Not applicable.

Funding

This work was funded by the Research Personnel Cultivation Programme of Zhongda Hospital Southeast University (No. CZXM-GSP-RC51).

Conflict of Interest

The authors declare no conflicts of interest.



References

- [1] Izzy S. Traumatic Spinal Cord Injury. Continuum (Minneapolis, Minn.). 2024; 30: 53–72. https://doi.org/10.1212/CON. 0000000000001392.
- [2] Jin LY, Li J, Wang KF, Xia WW, Zhu ZQ, Wang CR, et al. Blood-Spinal Cord Barrier in Spinal Cord Injury: A Review. Journal of Neurotrauma. 2021; 38: 1203–1224. https://doi.org/10.1089/ne u.2020.7413.
- [3] Hersh AM, Weber-Levine C, Jiang K, Theodore N. Spinal Cord Injury: Emerging Technologies. Neurosurgery Clinics of North America. 2024; 35: 243–251. https://doi.org/10.1016/j. nec.2023.10.001.
- [4] Schreiner TG, Schreiner OD, Ciobanu RC. Spinal Cord Injury Management Based on Microglia-Targeting Therapies. Journal of Clinical Medicine. 2024; 13: 2773. https://doi.org/10.3390/jc m13102773.
- [5] Guan P, Fan L, Zhu Z, Yang Q, Kang X, Li J, et al. M2 microglia-derived exosome-loaded electroconductive hydrogel for enhancing neurological recovery after spinal cord injury. Journal of Nanobiotechnology. 2024; 22: 8. https://doi.org/10. 1186/s12951-023-02255-w.
- [6] Xu A, Yang Y, Shao Y, Jiang M, Sun Y, Feng B. FHL2 regulates microglia M1/M2 polarization after spinal cord injury via PARP14-depended STAT1/6 pathway. International Immunopharmacology. 2023; 124: 110853. https://doi.org/10.1016/j.intimp.2023.110853.
- [7] Chen W, Gao X, Yang W, Xiao X, Pan X, Li H. Htr2b Promotes M1 Microglia Polarization and Neuroinflammation after Spinal Cord Injury via Inhibition of Neuregulin-1/ErbB Signaling. Molecular Neurobiology. 2024; 61: 1643–1654. https://doi.org/10.1007/s12035-023-03656-6.
- [8] Di Stadio A, Angelini C. Microglia polarization by mitochondrial metabolism modulation: A therapeutic opportunity in neurodegenerative diseases. Mitochondrion. 2019; 46: 334–336. https://doi.org/10.1016/j.mito.2018.09.003.
- [9] Ji H, Chu W, Yang Y, Peng X, Song X. Conditioned culture medium of bone marrow mesenchymal stem cells promotes phenotypic transformation of microglia by regulating mitochondrial autophagy. PeerJ. 2024; 12: e17664. https://doi.org/10.7717/pe erj.17664.
- [10] Jones EV, Bernardinelli Y, Zarruk JG, Chierzi S, Murai KK.

- SPARC and GluA1-Containing AMPA Receptors Promote Neuronal Health Following CNS Injury. Frontiers in Cellular Neuroscience. 2018; 12: 22. https://doi.org/10.3389/fncel.2018.
- [11] Lloyd-Burton SM, York EM, Anwar MA, Vincent AJ, Roskams AJ. SPARC regulates microgliosis and functional recovery following cortical ischemia. The Journal of Neuroscience: the Official Journal of the Society for Neuroscience. 2013; 33: 4468– 4481. https://doi.org/10.1523/JNEUROSCI.3585-12.2013.
- [12] Thomas SL, Schultz CR, Mouzon E, Golembieski WA, El Naili R, Radakrishnan A, et al. Loss of Sparc in p53-null Astrocytes Promotes Macrophage Activation and Phagocytosis Resulting in Decreased Tumor Size and Tumor Cell Survival. Brain Pathology (Zurich, Switzerland). 2015; 25: 391–400. https://doi.org/10.1111/bpa.12161.
- [13] Kumar M, Sharma S, Kumar J, Barik S, Mazumder S. Mito-chondrial electron transport chain in macrophage reprogramming: Potential role in antibacterial immune response. Current Research in Immunology. 2024; 5: 100077. https://doi.org/10.1016/j.crimmu.2024.100077.
- [14] O'Neill LAJ, Kishton RJ, Rathmell J. A guide to immunometabolism for immunologists. Nature Reviews. Immunology. 2016; 16: 553–565. https://doi.org/10.1038/nri. 2016.70.
- [15] Kelly B, O'Neill LAJ. Metabolic reprogramming in macrophages and dendritic cells in innate immunity. Cell Research. 2015; 25: 771–784. https://doi.org/10.1038/cr.2015.68.
- [16] Mills EL, Kelly B, Logan A, Costa ASH, Varma M, Bryant CE, et al. Succinate Dehydrogenase Supports Metabolic Repurposing of Mitochondria to Drive Inflammatory Macrophages. Cell. 2016; 167: 457–470.e13. https://doi.org/10.1016/j.cell.2016.08.064
- [17] Degterev A, Huang Z, Boyce M, Li Y, Jagtap P, Mizushima N, et al. Chemical inhibitor of nonapoptotic cell death with therapeutic potential for ischemic brain injury. Nature Chemical Biology. 2005; 1: 112–119. https://doi.org/10.1038/nchembio711.
- [18] Orihuela R, McPherson CA, Harry GJ. Microglial M1/M2 polarization and metabolic states. British Journal of Pharmacology. 2016; 173: 649–665. https://doi.org/10.1111/bph.13139.
- [19] Zhou R, Yazdi AS, Menu P, Tschopp J. A role for mitochondria in NLRP3 inflammasome activation. Nature. 2011; 469: 221– 225. https://doi.org/10.1038/nature09663.

